A dual role for the immune response in a mouse model of inflammation-associated lung cancer

Michael Dougan,[1,2] Danan Li,[1] Donna Neuberg,[3] Martin Mihm,[4] Paul Googe,[5] Kwok-Kin Wong,[1] and Glenn Dranoff[1,2]

[1]Department of Medical Oncology and [2]Cancer Vaccine Center, Dana-Farber Cancer Institute, and Department of Medicine, Brigham and Women's Hospital and Harvard Medical School, Boston, Massachusetts, USA. [3]Department of Biostatistics and Computational Biology, Dana-Farber Cancer Institute, and Department of Biostatistics, Harvard School of Public Health, Boston, Massachusetts, USA. [4]Department of Dermatology, Brigham and Women's Hospital and Harvard Medical School, Boston, Massachusetts, USA. [5]Knoxville Dermatopathology Laboratory, Knoxville, Tennessee, USA.

Lung cancer is the leading cause of cancer death worldwide. Both principal factors known to cause lung cancer, cigarette smoke and asbestos, induce pulmonary inflammation, and pulmonary inflammation has recently been implicated in several murine models of lung cancer. To further investigate the role of inflammation in the development of lung cancer, we generated mice with combined loss of IFN-γ and the β-common cytokines GM-CSF and IL-3. These immunodeficient mice develop chronic pulmonary inflammation and lung tumors at a high frequency. Examination of the relationship between these tumors and their inflammatory microenvironment revealed a dual role for the immune system in tumor development. The inflammatory cytokine IL-6 promoted optimal tumor growth, yet wild-type mice rejected transplanted tumors through the induction of adaptive immunity. These findings suggest a model whereby cytokine deficiency leads to oncogenic inflammation that combines with defective antitumor immunity to promote lung tumor formation, representing a unique system for studying the role of the immune system in lung tumor development.

Introduction

Lung cancer is the leading cause of malignant death for both men and women worldwide (1). Approximately 80% of lung tumors are non–small cell lung cancers (NSCLCs), which are further subdivided into squamous cell carcinomas and adenocarcinomas. The overall prognosis for NSCLC is poor, with a 5-year survival around 15% (2). Chronic carcinogen exposure, primarily in the form of cigarette smoke, is by far the largest contributing factor to the development of lung cancer (3). Yet other factors are doubtlessly involved, given that many smokers never develop malignant disease and that lung cancer arises in individuals without known risk factors (4). Several oncogenes and tumor suppressors are known to play important roles in lung cancer formation. Mutations in *p53* and *KRAS* are frequently observed in smoking-related lung tumors, and a substantial fraction of non-smoking-related adenocarcinomas express a mutated, constitutively active form of EGFR (5).

A variety of systems have been used to model human lung cancer in mice (6, 7). Although murine models of carcinogen-induced lung cancer have been developed, most murine models of lung cancer rely on genetic manipulation, with most current genetic models generating spontaneous lung tumors through germline manipulations in known oncogenes, including *Kras* and *Egfr*, or tumor suppressors such as *p53* (6–9).

Increasingly, chronic inflammation is being recognized as an important contributing factor to the development of a wide range of malignancies, and inflammation induced by microbial infection now appears to be the primary cause of most cancers of the stomach and liver (10). Although no direct link between inflammation and lung cancer has been established in humans, the most important environmental factors known to predispose to lung cancer, cigarette smoke and asbestos, produce pulmonary inflammation (11); furthermore, smoking-associated inflammation and activation of NF-κB pathways have been linked to lung cancer in both genetic and carcinogen-induced models (12). As is the case with several types of cancer, long-term use of antiinflammatory compounds correlates with a reduced incidence of lung cancer (13, 14). In human lung cancer cells, activation of EGFR signaling can induce production of the inflammatory cytokine IL-6, which serves as an autocrine growth factor for these tumors (15). Similarly, bronchoalveolar carcinoma can be induced in mice by pulmonary epithelial expression of a constitutively activated form of STAT3, a central signaling molecule downstream of IL-6 and related cytokines (16, 17); these mice develop chronic pulmonary inflammation, although whether this contributes to tumor growth is currently unclear (17).

More recent evidence supports a role for multiple inflammatory pathways in lung cancer development (18–21). An important role for NF-κB signaling has been demonstrated in distinct models of lung cancer, and the noncanonical IκB kinase TBK has been shown to be critical for the survival of human lung cancer cell lines expressing mutant K-ras (18–20). In addition, neutrophil elastase has been shown to promote IRS-1 degradation and tumor growth in a K-ras–dependent lung tumor model (21).

We previously reported a novel lymphoma model similar to human mucosa-associated lymphoid tissue (MALT) lymphomas based on combined deficiency in IFN-γ and the β-common cytokines GM-CSF and IL-3 in C57BL/6 (BL6) mice (triple-knockout [TKO] mice) (22). Both GM-CSF– and GM-CSF/IL-3–deficient animals have defects in the clearance of apoptotic cells associated with loss of the secreted phosphatidylserine-binding protein milk fat globule–epidermal growth factor–8 (MFG-E8) (22, 23). When

Conflict of interest: The authors have declared that no conflict of interest exists.
Citation for this article: *J Clin Invest.* 2011;121(6):2436–2446. doi:10.1172/JCI44796.

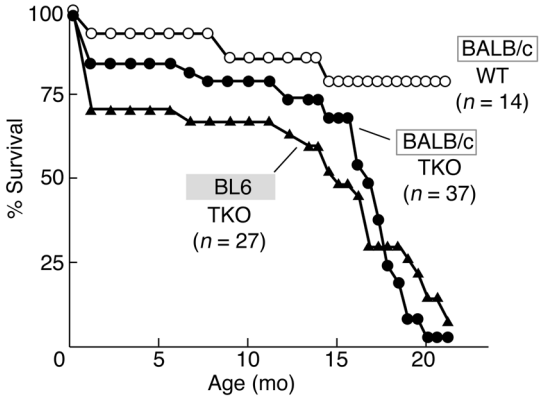

Figure 1
BALB/c TKO mice develop lung cancer. Survival curves compare BALB/c WT (n = 14), BALB/c TKO (n = 37), and BL6 TKO (n = 27) mice.

exposed to apoptotic cells, phagocytes from GM-CSF–deficient animals show excess production of inflammatory cytokines including IL-1β and IL-6 (23). In GM-CSF–deficient animals, this inappropriate response to apoptotic cells is associated with a decrease in Tregs and development of autoimmune pathologies including lupus and type 1 diabetes (22–24). Additional loss of IFN-γ in GM-CSF/IL-3–deficient mice leads to Th17 skewing, as well as increased susceptibility to infection (22–24). On the BL6 background, chronic infection, inflammation, and Th17 skewing are associated with a dramatic rise in the incidence of B cell lymphoma; between the ages of 12 and 16 months, approximately 80% of BL6 TKO mice develop lymphomas (22). In addition to lymphomas, some of these mice also develop solid tumors, including tumors of the ovaries and pancreatic islets. Intriguingly, these tumors are prevented by prophylactic broad spectrum antibiotics (Baytril), establishing a causative role for microflora in this system (22).

Approximately 40% of BL6 TKO mice die during the first month of life due to inflammation associated with the normal pulmonary flora, and all of the mice develop chronic pulmonary inflammation and pulmonary alveolar proteinosis (PAP). Despite the severe pulmonary inflammation found in BL6 TKO mice, these animals do not develop lung cancer (22). The BL6 background is known to be relatively resistant to several models of lung cancer, including carcinogen-induced lung cancer models (6). Although the precise genetic mechanism leading to resistance has yet to be established, polymorphisms in the pulmonary adenocarcinoma susceptibility 1 (*Pas1*) locus near the *Kras2* gene have been identified as an important susceptibility factor in several sensitive strains, including BALB/c (6, 25). The well-established resistance of BL6 mice to lung cancer suggests that this may not be the appropriate background for studying the contribution of inflammation to lung cancer development.

Here we found that, when BL6 TKO mice were crossed onto the lung cancer–susceptible BALB/c background, the combination of GM-CSF, IL-3, and IFN-γ deficiency led to the development of invasive pulmonary adenocarcinomas. These tumors arose with high penetrance, occurred in the context of chronic pulmonary inflammation and infection, and displayed many features of other models of lung cancer, including an association with dysplastic lesions and spontaneous activation of MAPK and STAT3 signaling, in addition to a critical dependence on NF-κB signaling.

We further show that, consistent with a role for chronic inflammation in the onset of these adenocarcinomas, the inflammatory cytokine IL-6 acted as an autocrine growth factor in this system, and restoration of immune function reduced lung cancer incidence. In addition, both IL-6 and the tumor-promoting cytokine IL-17 were overexpressed in BALB/c TKO mice, and T cells derived from these animals produced increased levels of both cytokines. However, the immune system appears to play a dual role in the genesis of lung tumors in BALB/c TKO mice, as transplanted adenocarcinomas could be rejected by immunocompetent recipients but not by immunodeficient hosts. Taken together, these findings suggest that the tumors in this system arise through a combination of tumor-promoting inflammation and failure of spontaneous antitumor immunity. These results establish a model of lung cancer initiated by alterations in immune response genes in the absence of germline mutations in known oncogenes or tumor suppressors.

Results

BALB/c TKO mice develop invasive pulmonary adenocarcinomas. To examine the influence of strain type on the distribution of tumors arising spontaneously in TKO mice, we bred BL6 TKO animals onto the BALB/c background; efficiency of back-crossing was confirmed by commercially available single nucleotide polymorphism analysis (Taconic) and demonstrated 98.4% BALB/c genomic content (data not shown). Similar to BL6 TKO animals, BALB/c TKO mice displayed increased mortality after 12 months of age (BALB/c WT versus TKO, $P < 0.0001$) (Figure 1). Yet unlike BL6 mice, older BALB/c TKO mice succumbed largely to pulmonary disease, with 100% of animals older than 1 year of age harboring invasive pulmonary tumors resembling adenocarcinomas (Table 1). Although the mechanism underlying the resistance of BL6 mice to these lung tumors is still unclear, lung tumors were present in BL6 × BALB/c TKO F_1 hybrids, indicating the presence of at least one dominant susceptibility gene in the BALB/c genome (data not shown).

Spontaneous lung tumors have been reported in a small fraction of BALB/c mice deficient in IFN-γ, with tumors arising around 2 years of age (26). The highly penetrant tumors arising in BALB/c TKO mice required deficiency in both GM-CSF/IL-3 and IFN-γ and were not present in age-matched, 12-month-old WT, IFN-γ–deficient, or GM-CSF/IL-3 double-deficient (DKO) mice (Table 1). As was observed in BL6 TKO mice, lymphomas arose in a proportion of BALB/c TKO animals; however, unlike the pulmonary tumors, the prevalence of lymphoma was highly variable depending on the cohort and did not occur in all facilities in which the animals were housed (data not shown). This finding suggests a role for specific microflora in the promotion of these lymphomas, which is consistent with the efficacy of prophylactic antibiotics in BL6 TKO mice.

BALB/c TKO animals experience chronic pulmonary inflammation and pneumonia that was evident even in young, 2- to 3-month-old animals (Figure 2, A and B). Over a period of several months, this inflammation was associated with the development of epithelial dysplasia that resembled early premalignant lesions found in other models of lung cancer (Figure 2C) (6). By 6–9 months of age, more than half of the mice harbored frank pulmonary malignancies (Figure 2D). Consistent with their morphologic resemblance to adenocarcinoma, these tumors expressed surfactant protein C (SPC), a common marker of pulmonary adenocarcinoma in both mice and humans (Figure 2E); as expected, these tumors were negative for the small cell lung cancer marker clara cell antigen (CCA) (data not shown).

Table 1
Frequency of lung cancer by genotype

Genotype	Mice with lung cancer/total[A]
WT	0/9
TKO	24/24
DKO	0/15
IFN-$\gamma^{-/-}$	0/8

[A]All mice were sacrificed at 12–14 months of age; lungs were examined by histopathology for the presence of lung cancer.

As discussed earlier, activation of K-ras and EGFR signaling is a common feature in distinct subsets of human lung cancer, and genetic manipulation of either of these pathways can produce pulmonary adenocarcinoma in mice (6–9). Given the resemblance to pulmonary adenocarcinoma, we hypothesized that the tumors arising in BALB/c TKO mice would have acquired changes in oncogene activation characteristic of lung cancer in other systems. In order to test this hypothesis, we examined EGFR and K-ras signaling in primary BALB/c TKO tumor sections and in cell lines derived from primary tumors. Although EGFR activation as measured by the levels of EGFR and phosphorylated EGFR (pEGFR) was not apparent in either primary samples or cell lines (data not shown), BALB/c TKO tumors did show evidence of high levels of pERK, a downstream target of K-ras in the MAPK cascade that is frequently activated in lung cancer (Figure 2F). Mutations in *Kras* itself have not yet been detected in any of the BALB/c TKO–derived tumor cell lines examined, suggesting that MAPK signaling may be activated by a distinct mechanism in this system.

These findings indicate that, even without germline changes in oncogene expression, the tumors that arise in BALB/c TKO mice recapitulate aspects of lung tumor development found in other models, including human lung tumors. The resemblance to human lung tumors is further emphasized by the development of invasive lesions in BALB/c TKO mice that can give rise to distant metastases with both hematologic and lymphatic spread, as well as growth in the liver and kidneys evident in a portion of animals (Figure 2, G and H, and data not shown). These metastases maintain scattered expression of SPC, as well as pERK, confirming their relationship to the primary pulmonary tumors (Supplemental Figure 1; supplemental material available online with this article; doi:10.1172/JCI44796DS1).

BALB/c TKO lung tumors occur in the context of chronic inflammation. In order to investigate the role for hematopoietic cells in the onset of BALB/c TKO lung tumors, we generated bone marrow chimeras in which lethally irradiated 6- to 8-week-old TKO mice were reconstituted with WT bone marrow and followed for 1 year. Although tumors or dysplastic lesions were evident in control TKO animals reconstituted with TKO marrow (n = 3: 2 tumors, 1 dysplastic lesion), pulmonary inflammation and lung tumor development were suppressed in animals receiving WT marrow (n = 4), consistent with a role for hematopoietic cells in the onset of these tumors (Table 2).

Isolated hematopoietic deficiency in GM-CSF, IL-3, and IFN-γ was not sufficient to promote lung tumor formation. The lungs from lethally irradiated WT mice reconstituted with TKO bone marrow were indistinguishable from lungs taken from control animals reconstituted with WT marrow (n = 4 for each group) (Table 2). This finding is not surprising, given that pulmonary epithelial cells, which are radiation resistant, can produce GM-CSF in sufficient quantities to correct the defect in pulmonary homeostasis in GM-CSF–deficient mice (27).

Based on this finding, we decided to further investigate the relationship between inflammation and tumor development in this system, beginning with the characterization of the inflammatory microenvironment in the BALB/c TKO lung. While BALB/c TKO mice showed a slight increase in total spleen cells, indicative of mild systemic inflammation, the inflammation in the lungs was disproportionately more severe (Figure 3A and Supplemental Figure 2). Even by 2–3 months of age, BALB/c TKO mice exhibited severe pulmonary inflammation characterized by pulmonary infiltrates that contain B cells and T cells, granulocytes, macrophages, and Gr-1$^+$CD11b$^+$ myeloid cells (Figure 3A). These Gr-1$^+$CD11b$^+$ cells displayed a surface phenotype overlapping with myeloid suppressor cells, although whether these cells had a true immune-suppressive phenotype remains to be established.

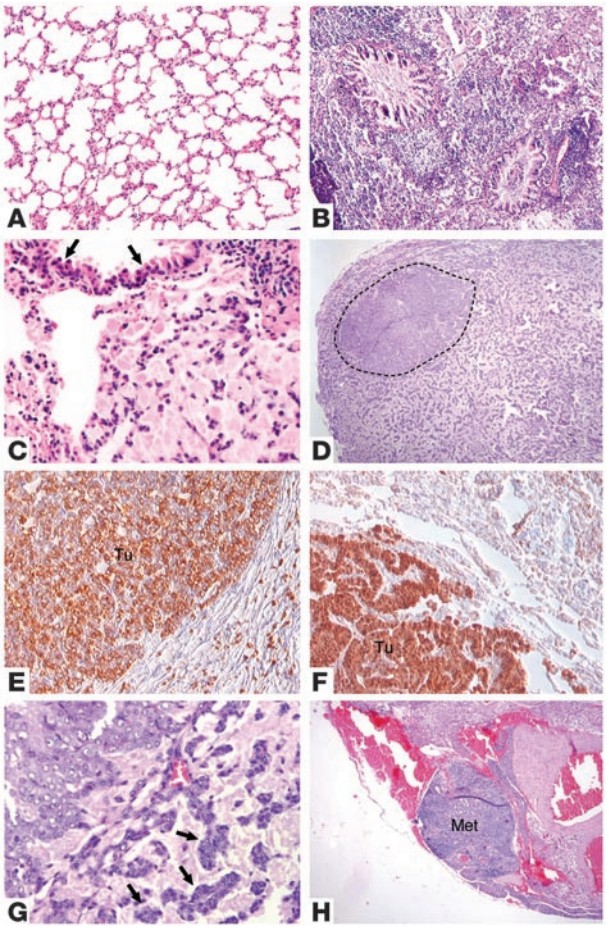

Figure 2
BALB/c TKO lung tumors are invasive pulmonary adenocarcinomas. (**A**–**D**) H&E stains on formalin-fixed tissue sections. One-year-old WT (**A**) and TKO (**B**) lung (original magnification, ×40). (**C** and **D**) TKO lung showing a dysplastic lesion (**C**; ×400) in a 6-month-old mouse and invasive pulmonary adenocarcinoma (**D**; ×20) in a 14-month-old animal. Arrows in **C** indicate dysplastic epithelium. SPC (**E**) and pERK (**F**) immunohistochemistry (×100) on BALB/c TKO pulmonary adenocarcinoma from 16-month-old (**E**) and 12-month-old (**F**) mice. The tumor (Tu) is indicated. (**G** and **H**) H&E staining showing invasion (**G**; ×100) indicated by the arrows and thoracic lymph node metastasis (Met) (**H**; ×20) in a 15-month-old mouse; **G** shows a detail from **D**.

Table 2
Lung cancer prevalence in bone marrow chimeric mice

Genotype		
Donor	Recipient	Mice with lung cancer/total[A]
WT	WT	0/4
WT	TKO	0/4
TKO	WT	0/4
TKO	TKO	3/3

[A]All mice were sacrificed at 12 months of age (10 months after transplantation); lungs were examined by histopathology for the presence of lung cancer.

Many chronic inflammatory reactions are linked to tumor development through the production of inflammatory cytokines, including TNF-α, IL-1β, IL-6, and IL-17 (28–31). We hypothesized that one or several of these cytokines may be present in the airways of younger BALB/c TKO animals, particularly given that we had previously shown dysregulation in the production of these cytokines following recognition of apoptotic cells by BL6 TKO–derived antigen-presenting cells (23). To detect pulmonary cytokine secretion, we performed BAL on BALB/c TKO and WT mice and measured cytokine levels in the lavage fluid. Significant elevations in BAL fluid IL-6 ($P = 0.002$) and TNF-α ($P = 0.04$) were evident in TKO mice compared with controls (Figure 3B). Both of these cytokines, along with IL-17, were elevated in the sera of BALB/c TKO mice (IL-6, $P = 0.009$; TNF-α, $P = 0.004$; IL-17, $P = 0.05$); however, for IL-6 the difference between TKO and WT animals was substantially greater in the BAL fluid (Figure 3B). The presence of disproportionately high levels of IL-6 in the pulmonary microenvironment indicates a potential role for this cytokine in the subsequent development of adenocarcinoma. Furthermore, as BALB/c TKO mice aged, increasingly high levels of IL-6 became detectable in the serum, with the highest levels in mice greater than 1 year of age, a point at which all of the mice had been found to harbor cancer (Figure 3C). The correlation between systemic IL-6 and the presence of lung tumors hints at a possible direct role for these tumors in IL-6 production. To further investigate the role of IL-6 in the pulmonary microenvironment, IL-6 signaling measured by pSTAT3 was examined in the lungs of 2-month-old TKO mice. By immunohistochemistry, BALB/c TKO mice showed nuclear pSTAT3 in the pulmonary airway epithelium in 2 of 4 animals examined; similar staining was not evident in aged-matched WT mice ($n = 4$) (data not shown).

Although IL-6 was notably increased in aged BALB/c TKO mice, IL-6 was not the only elevated tumor-promoting cytokine in these animals. IL-17 levels were significantly increased in 1-year-old BALB/c TKO mice compared with age-matched WT animals ($P = 0.004$), suggesting that multiple tumor-promoting inflammatory pathways may be acting in parallel in this system (Figure 3D).

The elevated levels of tumor-promoting cytokines present in BALB/c TKO serum and BAL fluid could relate to an underlying tendency toward increased inflammatory cytokine production in these animals. Consistent with earlier reports in BL6 mice, we found that stimulated BALB/c TKO $CD4^+$ T cells produced a skewed cytokine profile compared with WT, with elevated levels of both IL-6 and IL-17 in addition to generally increased levels of Th2-type cytokines (IL-6, $P = 0.004$; IL-17, $P = 0.04$) (Figure 3E, Supplemental Figure 3, and refs. 22, 23). In contrast to IL-6 and IL-17, differences in TNF-α secretion were not observed, and IL-1β was not produced at detectable levels by either TKO or WT T cells (Figure 3E and data not shown). These findings suggest that cytokines produced from pulmonary infiltrating T cells may, in part, account for the elevated levels of tumor-promoting cytokines observed in the BAL fluid. Furthermore, Th2 skewing more generally may promote tumor growth, as Th2 responses have recently been linked to enhanced tumor invasion and metastasis through effects on $Gr\text{-}1^+CD11b^+$ myeloid cell function (32).

Macrophage chemokine production also differed between BALB/c WT and TKO mice. Cultured macrophages from TKO mice produced substantially elevated levels of the inflammatory chemokine IFN-γ–induced protein–10 (IP-10) in combination with decreased secretion of the Treg chemotactic factor CCL22 ($P = 0.002$ for both chemokines) (Figure 3F, Supplemental Figure 3, and ref. 23). More subtle, though statistically significant, decreases in the chemokines KC and macrophage inflammatory protein 2 (MIP-2), as well as increased secretion of chemokine MIP-1β, were also observed, though the biological relevance of these small differences is difficult to discern ($P = 0.002$ for all 3 chemokines) (Supplemental Figure 3). Functional Tregs have been shown to inhibit tumor growth in other models of inflammation-driven cancer, suggesting that deficient Treg recruitment due to decreased CCL22 secretion from BALB/c TKO macrophages coupled with inflammatory chemokine production may further support tumor growth (33).

BALB/c TKO lung tumors secrete IL-6 and provoke an inflammatory response in secondary hosts. Given the evidence linking BALB/c TKO–derived lung tumors to an inflammatory microenvironment, and to IL-6 in particular, we next sought to examine the ability of these tumors to secrete inflammatory mediators directly. In order to study these tumors in isolation, we established a series of cell lines derived from primary lung tumors. We then selected two of these tumors (MDAC1 and MDAC8) to study in more detail, using a 21-cytokine detection panel to survey cytokine secretion by these cell lines.

The two lung tumors produced a similar set of cytokines, including the chemokines KC, monocyte chemotactic protein–1 (MCP-1), and MIP-1β, the angiogenic factor VEGF, and IL-6. VEGF has been implicated in lung tumor formation in other systems and is secreted by many mouse tumor cell lines, including the lung tumor line Lewis lung (LL) (Figure 4A). IL-6 secretion was confirmed by ELISA in a panel including several additional freshly isolated BALB/c TKO lung tumors, and was not found at high levels in other mouse tumor cell lines examined, including LL (Figure 4A and data not shown). Furthermore, IL-6 secretion was not dependent on tumor-associated macrophages, as IL-6 was readily detectable in tumor cultures in which the small population of $CD11b^+$ cells had been removed (data not shown). Collectively, these findings suggest a model in which immune dysregulation in young animals, likely following from deficiencies in MFG-E8–mediated uptake of apoptotic cells, produces an inflammatory pulmonary microenvironment rich in IL-6 (23). As tumors develop, selective pressure promotes the emergence of tumors with the capacity for autocrine IL-6 production; evidence indicating strong selective pressure for the production of IL-6 by tumor cells is presented below (Figure 5).

The majority of BALB/c TKO–derived lung tumors could not be maintained in tissue culture, yet we were able to establish several cell lines that propagate as either subcutaneous or intrapulmonary masses in secondary hosts, confirming the malignancy of the primary tumors. Upon transplantation into secondary hosts, BALB/c TKO tumors provoked an unexpectedly vigorous inflammatory

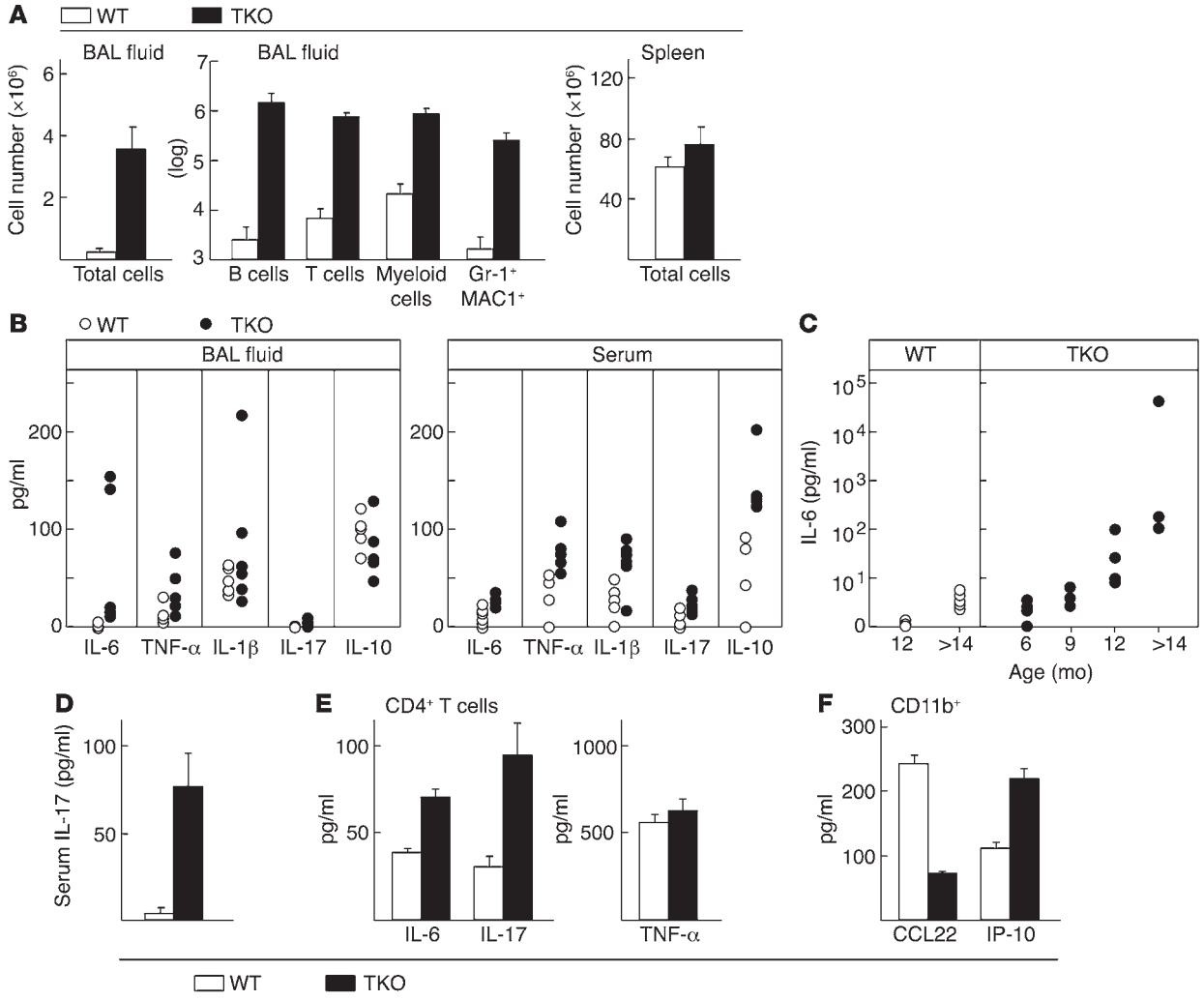

Figure 3

BALB/c TKO lung tumors develop in the context of pulmonary and systemic inflammation. (**A**) Comparison of total leukocytes recovered from BAL fluid from 3-month-old BALB/c TKO and WT mice (left panel) and analysis of lymphoid and myeloid subtypes (middle panel) using flow cytometry. Right panel: Total spleen cells from the same WT and TKO mice are presented for comparison. (**B**) Quantification of inflammatory cytokines present in the BAL fluid (left panel) and serum (right panel) of 3-month-old BALB/c TKO and WT mice; each point represents an individual animal. Cytokines were measured using fluorescent anti-cytokine beads; IL-6 levels in the BAL fluid were confirmed by ELISA. Results represent an analysis of samples collected from 3 independent experiments. (**C** and **D**) Quantification of serum cytokines in aged BALB/c WT and TKO mice by ELISA. (**C**) Points represent individual animals. (**D**) Serum IL-17 in 1-year-old WT (n = 6) and TKO (n = 4) mice. (**E** and **F**) Cytokine production from 1 × 10^6 $CD4^+$ T cells (**E**) stimulated for 48 hours using anti-CD3 (10 μg/ml) and anti-CD28 (2 μg/ml), or from $CD11b^+$ macrophages (**F**) cultured for 18 hours. Cells were isolated from spleens of 6- to 8-week-old mice by positive selection with magnetic beads (Miltenyi Biotec). Cytokines/chemokines were measured using anti-cytokine beads. Results are combined from 2 independent experiments with a total of 6 (**E**) or 4 (**F**) mice per group. Error bars represent SEM.

response, characterized by the formation of large cystic structures and a substantial influx of macrophages and neutrophils, as well as T cells and B cells (Figure 4, B and C). These inflammatory reactions were observable in both WT and TKO hosts, and for some cell lines represented the majority of the tumor mass. In WT mice, transplantation of TKO-derived tumor cell lines, including MDAC8, was associated with a systemic expansion of immune cells, characterized by enlarged spleens and lymph nodes and increases in both innate and adaptive immune cells; this expansion was most evident among B cells and granulocytes (Figure 4D and data not shown). These findings indicate that the inflammatory mediators secreted by the BALB/c TKO tumors, in particular IL-6, serve to recapitulate the favorable inflammatory microenvironment in which the tumors initially arose.

Knockdown of IL-6 in BALB/c TKO lung tumor cell lines reduces ERK and STAT3 activation and slows tumor growth. Due to consistent IL-6 secretion by BALB/c TKO tumors, we hypothesized that IL-6 could be acting as an autocrine growth factor in this system. In order to directly assess the importance of IL-6 to BALB/c TKO lung tumor growth, we generated cell lines stably transfected with lentiviral vectors encoding shRNAs directed against IL-6. A panel of 5 shRNAs was examined and two, representing the least (KD-1) and most (KD-2) effective constructs, were selected for extensive evaluation (Figure 5A and data not shown).

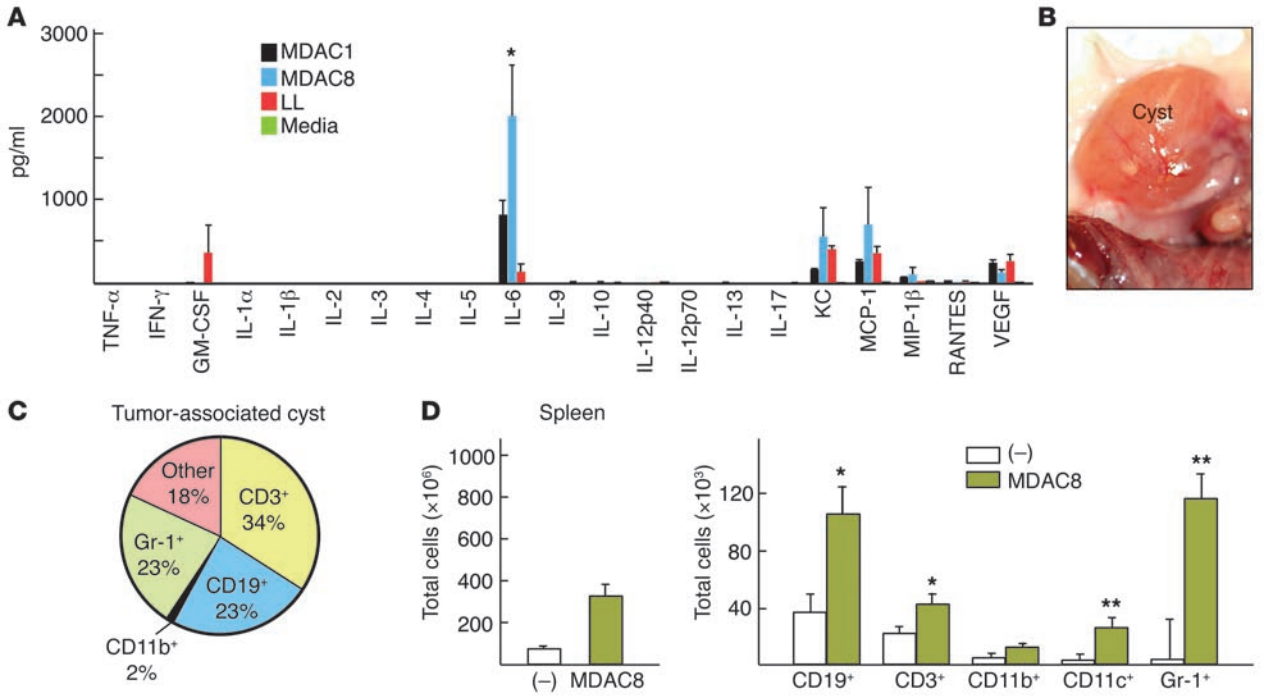

Figure 4

Transplanted BALB/c TKO tumor cell lines elicit a vigorous host response. (**A**) Analysis of cytokine secretion by BALB/c TKO lung tumor cells lines (MDAC1, MDAC8) using anti-cytokine fluorescent beads. *$P < 0.05$, MDAC8 compared with LL (**B**) Cyst associated with a transplanted BALB/c TKO lung tumor. (**C**) Analysis of cyst contents by flow cytometry using the indicated antibodies; numbers are an average from 2 tumor-associated cysts harvested from separate animals. (**D**) Quantification of immune cell expansion in the spleens of mice harboring transplanted BALB/c TKO tumors. Cell types were identified by flow cytometry. Results are combined from 3 independent experiments with 2–3 animals per group. Error bars represent SEM. *$P < 0.05$, **$P < 0.005$, MDAC8-injected compared with control (–) animals.

IL-6 is known to activate MAPK and STAT3 signaling, and activation of both of these pathways has been implicated in tumor growth in a variety of systems (16). We had previously demonstrated high levels of pERK1/2, a downstream target in the MAPK pathway, in primary BALB/c TKO tumors (Figure 2G); consistent with an important role for IL-6 in the activation of this pathway in BALB/c TKO lung tumors, knockdown of IL-6 was associated with a substantial decrease in pERK1/2 levels (Figure 5B). In addition, levels of nuclear STAT3 were also decreased in IL-6 knockdown tumors, indicating a role for autocrine IL-6 in both pathways (Figure 5B).

In cells expressing KD-2, reduction in both signaling pathways was associated with diminished growth capacity in culture (nontargeting shRNA vs. KD-2: $P < 0.0001$) (Figure 5C). After transplantation into 6- to 8-week-old BALB/c TKO mice, KD-2–expressing tumors showed decreased growth (nontargeting shRNA vs. KD-2: $P = 0.005$), which corresponded with improved survival in mice harboring these tumors (nontargeting shRNA vs KD-2: $P = 0.02$) (Figure 5D). Furthermore, cells isolated from KD-2–derived tumors grown in vivo showed substantial reactivation of IL-6 secretion, likely reflecting a combination of expansion of cells expressing low levels of the knockdown construct and infiltration of the tumor by IL-6–secreting host cells (Figure 5E).

Knockdown of IL-6 was associated with variable alterations in tumor-derived cytokine and chemokine secretion (Supplemental Figure 4). Secretion of VEGF was substantially increased in KD-2–expressing cells, as was the secretion of the inflammatory chemokines MCP-1 and LIX. In contrast, both IP-10 and MIP-1β were decreased in association with IL-6 knockdown (Supplemental Figure 4). No significant changes in MIP-1α, MIP-2, or KC secretion were found. Although the specific effects of these changes in cytokine secretion are difficult to determine, IL-6 knockdown clearly has a negative effect on tumor growth both in vitro and vivo. The substantial increase in VEGF secretion by knockdown cells may counteract some of the growth-limiting effects of IL-6 knockdown in vivo through enhanced angiogenesis; however, VEGF has also been shown to limit tumor invasion and metastasis (34, 35).

These results demonstrate a role for IL-6 in optimal tumor growth and further implicate oncogenic inflammation in the development of BALB/c TKO tumors. Similar autocrine IL-6 signaling has been shown to play a critical role in human lung tumors expressing EGFR; in this system, EGFR signaling led to IL-6 secretion and to activation of both MAPK and STAT3 pathways (15). Taken together, these findings suggest that autocrine IL-6 production may be a common feature of lung tumors with diverse origins.

BALB/c TKO tumor cell lines are susceptible to chemical inhibition of NF-κB signaling. Although IL-6 has a clear role in promoting optimal tumor growth in this system, elevated IL-6 signaling is unlikely to fully account for the increased risk of lung tumor formation in BALB/c TKO mice. As shown above, IL-17 was elevated in BALB/c TKO mice as well (Figure 3), and tumor cells directly produced VEGF in addition to multiple inflammatory chemokines (Figure 4 and Supplemental Figure 4). As discussed earlier, NF-κB has been

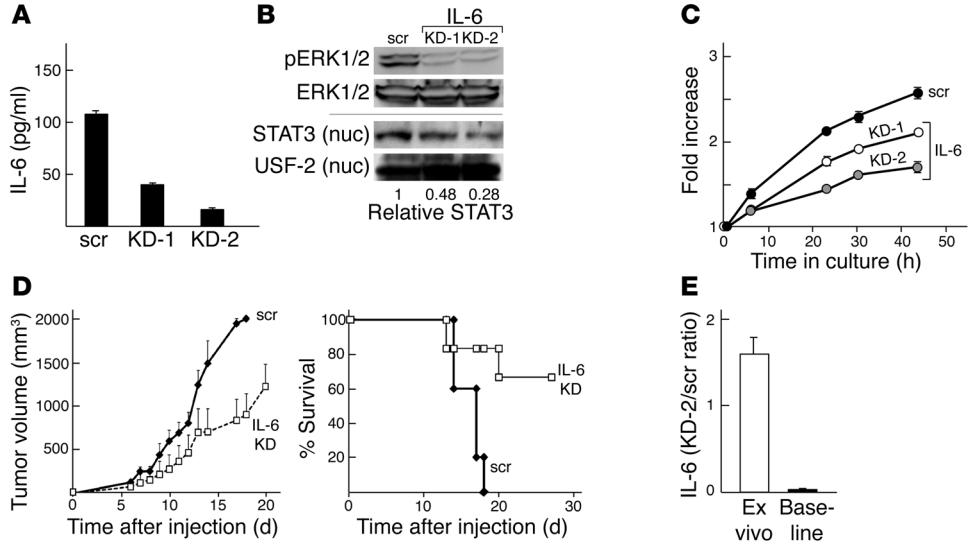

Figure 5

Knockdown of IL-6 reduces the proliferation of a BALB/c TKO lung tumor cell line. (**A**) 1×10^4 MDAC8 cells infected with lentiviruses encoding nontargeting shRNA (scr), or shRNA against IL-6 (KD-1 and KD-2) were cultured for 3 days in RPMI; supernatants were harvested, and total IL-6 was measured by ELISA. (**B**) Western blot for cytoplasmic pERK (top panels) or nuclear (nuc) STAT3 (bottom panels) using lysates from IL-6–knockdown or control (scr) MDAC8 cells. (**C** and **D**) In vitro (**C**) and in vivo (**D**) growth of MDAC8 cells expressing IL-6 shRNA compared with cells expressing nontargeting controls. (**C**) 1×10^4 cells were cultured in RPMI. Growth was measured by CellTiter-Glo (CTG, Promega). (**D**) Left panel: 4×10^4 cells were injected subcutaneously into BALB/c TKO mice, with 8 animals per group. Right panel: Survival of mice harboring tumors. (**E**) Comparison of IL-6 production from ex vivo cultured IL-6 KD-2 or control MDAC8 cell lines following growth in a secondary host (ex vivo) or after in vitro culture (baseline). Three to 4 tumors were used per group. (**A**–**E**) Results are representative of at least 2 independent experiments, with 6–8 replicates per experiment. Error bars represent the SEM for the experiment shown.

shown to promote tumor formation in models of smoking-related lung cancer; consequently, we wondered whether NF-κB activation might play a role in BALB/c TKO tumors.

Components of both NF-κB1 and NF-κB2 are readily detectable in nuclear protein fractions from MDAC8 cells (Figure 6A and Supplemental Figure 5). Confirming a critical function for NF-κB signaling in this system, combined inhibition of IκB kinase 1 (IKK1) and IKK2 using two chemically distinct inhibitors led to a rapid decrease in nuclear NF-κB p65 levels (Figure 6A) and corresponding loss of viability in treated cells ($P = 0.001$) (Figure 6B). Selective inhibitors of IKK2 were not effective at reducing nuclear NF-κB p65 (Figure 6A) and had no discernible effect on tumor cell viability (Figure 6B). Loss of cell viability was detectable within a day of treatment ($P = 0.001$ at 24 hours) (Figure 6C) and occurred in a dose-dependent fashion ($P < 0.0001$ for doses greater than 4 μM) (Figure 6D).

NF-κB can regulate the production of many inflammatory cytokines and chemokines. Thus, we next sought to determine the effect of IKK inhibition on cytokine secretion by BALB/c TKO tumor cells. IL-6 levels were decreased by all 4 inhibitors examined (compared with vehicle, $P = 0.001$ for all treatment conditions), demonstrating a role for NF-κB in the autocrine production of IL-6 in this system (Figure 6E). Similarly, IP-10 production was reduced by all 4 IKK inhibitors ($P = 0.0009$), and both LIX ($P = 0.02$) and VEGF ($P = 0.002$) secretion was reduced in cells treated with combined IKK1/2 inhibitors (Supplemental Figure 6); however, the specificity of this latter finding is difficult to determine given the poor overall viability associated with combined IKK1/2 inhibition. IL-6 knockdown did not influence susceptibility to either the combined IKK1/2 inhibitors or the selective IKK2 inhibitors (data not shown).

These findings suggest a critical role for NF-κB in the maintenance of BALB/c TKO tumor cells and indicate a role for NF-κB in the autocrine secretion of IL-6. The findings further suggest that NF-κB can play a role in diverse models of lung cancer, even in the absence of oncogene manipulation or frank carcinogen exposure.

Immunocompetent mice can reject transplanted BALB/c TKO tumors. IFN-γ has a well-established role in antitumor immune responses, with deficiency in IFN-γ associated with increased susceptibility to tumorigenesis in multiple models (10, 36, 37). Furthermore, STAT3 activation in tumor cells and in the tumor microenvironment has been shown to induce immune suppression that can limit antitumor immunity (16). Consequently, we wondered whether impaired antitumor responses could be further predisposing BALB/c TKO mice to lung cancer.

In order to examine the role of antitumor immunity in this system, we sought to determine whether BALB/c TKO–derived tumors would show signs of immune editing when transplanted into mice with intact immune responses. As had been observed in TKO transplant recipients, transplantation of BALB/c TKO lung tumors into WT mice elicited a vigorous host immune response characterized by infiltration with granulocytes, B cells, and both $CD4^+$ and $CD8^+$ T cells, with similar results found for both MDAC1 and MDAC8 (Figure 7A and data not shown).

Consistent with a role for immune editing in this system, BALB/c TKO tumors transplanted into BALB/c WT mice grew at a significantly slower rate than tumors transplanted into matched TKO animals ($P < 0.0001$) (Figure 7, B and C); furthermore, some WT animals failed to develop tumors altogether, while others reached an equilibrium state, maintaining tumor stasis for weeks (Figure 7C). Similar results were obtained with 3 tumor cell lines, including MDAC8, suggesting that the tumors that arise in BALB/c TKO mice are intrinsically immunogenic (data not shown).

Although these results are consistent with immune editing of transplanted tumors by WT immune cells, they may also reflect preference for growth in BALB/c TKO mice due to a favorable, inflammatory microenvironment. In order to distinguish between these possibilities, we established cell lines from transplanted tumors harvested from BALB/c WT (MDAC8.WT) or TKO (MDAC8.TKO) recipients. If the difference in growth rates

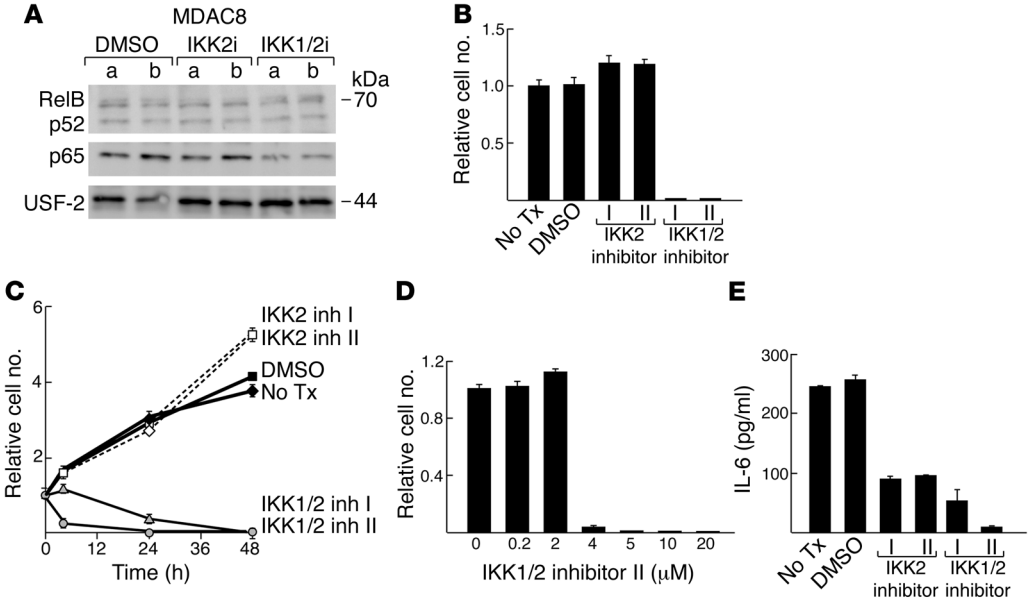

Figure 6

Inhibition of NF-κB signaling in a BALB/c TKO lung tumor cell line leads to rapid loss of viability. (**A**) Western blot of nuclear lysates from MDAC8 cells cultured for 1 hour with an IKK2 inhibitor (IKK2i), a combined IKK1-IKK2 inhibitor (IKK1/2i), or vehicle (DMSO); Data in **A** and **B** represent samples analyzed from 2 independent cultures. (**B**) 3×10^5 MDAC8 cells were cultured for 72 hours with IKK inhibitors, vehicle (DMSO), or media (No Tx); IKK2 inhibitor I is identical to IKK2i in **A**, and IKK1/2 inhibitor II is identical to IKK1/2i in **A**; relative cell numbers were determined using CTG, with the average reading for the untreated group defined as 1. (**C**) Time course of cell loss following IKK inhibitor treatment; cells were treated as in **B** and analyzed using CTG; the average reading for the untreated group at time 0 was defined as 1. (**D**) Dose response to IKK1/2 inhibitor II after 72 hours; cells were treated and analyzed as in **B**. (**E**) IL-6 production from MDAC8 cells treated with IKK inhibitors as in **B**; IL-6 was measured by ELISA. (**B**–**E**) Results are representative of 2–3 independent experiments, with 6 replicates per group. Error bars represent SEM. All IKK inhibitors were from EMD Biosciences and were used at the following concentrations unless otherwise indicated: IKK2 inhibitor I (EMD IKK-2 Inhibitor IV), 10 μM; IKK2 inhibitor II (EMD IKK-2 Inhibitor VI), 5 μM; IKK1/2 inhibitor I (BMS-345541), 40 μM; IKK1/2 inhibitor II (EMD IKK Inhibitor VII), 20 μM.

following transplantation into WT and TKO animals reflected an immune-mediated event, we would expect cell lines harvested from WT recipients to have undergone immune editing and to no longer show restricted growth in subsequent WT transplants. Conversely, if the slowed growth were primarily due to loss of a favorable inflammatory microenvironment, we would expect cells harvested from WT recipients to show growth characteristics similar to cells harvested from TKO animals. Consistent with a role for immune editing, tumor cells harvested from WT recipients showed substantially increased growth in subsequent WT transplants compared with cells harvested from TKO mice, despite indistinguishable growth rates in culture ($P < 0.0001$) (Figure 7, D and E).

In order to directly test the ability of adaptive immune cells to limit growth of BALB/c TKO–derived tumors, we next transplanted tumors into mice lacking adaptive immunity due to loss of recombination activating gene 2 (RAG-KO mice). As was observed in BALB/c TKO mice, tumors grew more rapidly in RAG-KO mice compared with WT controls ($P < 0.0001$) (Figure 7, F and G), indicating a role for adaptive immunity in tumor protection. These findings suggest that failure of immune editing of nascent tumors may account for part of the tumor susceptibility in BALB/c TKO mice (36, 37). Based on these findings, we hypothesized that loss of adaptive immune cells in BALB/c TKO mice could further accelerate tumor growth, and we generated mice deficient in GM-CSF, IL-3, IFN-γ, and RAG-2. These TKO RAG-KO mice rapidly developed overwhelming pneumonia, which precluded an assessment of lung cancer incidence, with most animals requiring sacrifice before reaching 3 months of age.

Discussion

Our results are consistent with a direct role for hematopoietic cells in the generation of lung cancer. Both myeloid and lymphoid cells are present in the tumor microenvironment, and restoration of normal immune function through bone marrow transplantation appears to prevent oncogenesis in this system. These findings further support a function for the immune system and inflammatory pathways in lung cancer development, as has been found in other models (12, 18–21).

Even in the absence of germline modifications in known oncogenes or tumor suppressors, the tumors that arise in BALB/c TKO mice share significant morphological and molecular similarities with other models of lung cancer, including activation of MAPK signaling and autocrine secretion of IL-6 (7, 8, 15). Much like adenocarcinoma in humans, the tumors arising in BALB/c TKO mice progress slowly over a period of months, beginning as microscopic lesions and eventually developing into large masses that metastasize to distant sites. The precise molecular events that distinguish these early tumors from the more advanced ones remain to be explored, but could be relevant to early events in human lung cancer development, since, in the absence of oncogenic manipulation, the pulmonary epithelium in BALB/c TKO mice more closely resembles the premalignant epithelium in humans.

In BALB/c TKO mice, tumor formation appears to begin with immune dysregulation. We have shown previously that loss of immune homeostasis in GM-CSF–deficient mice can be attributed, at least in part, to defects in the secretion of MFG-E8 and to a resul-

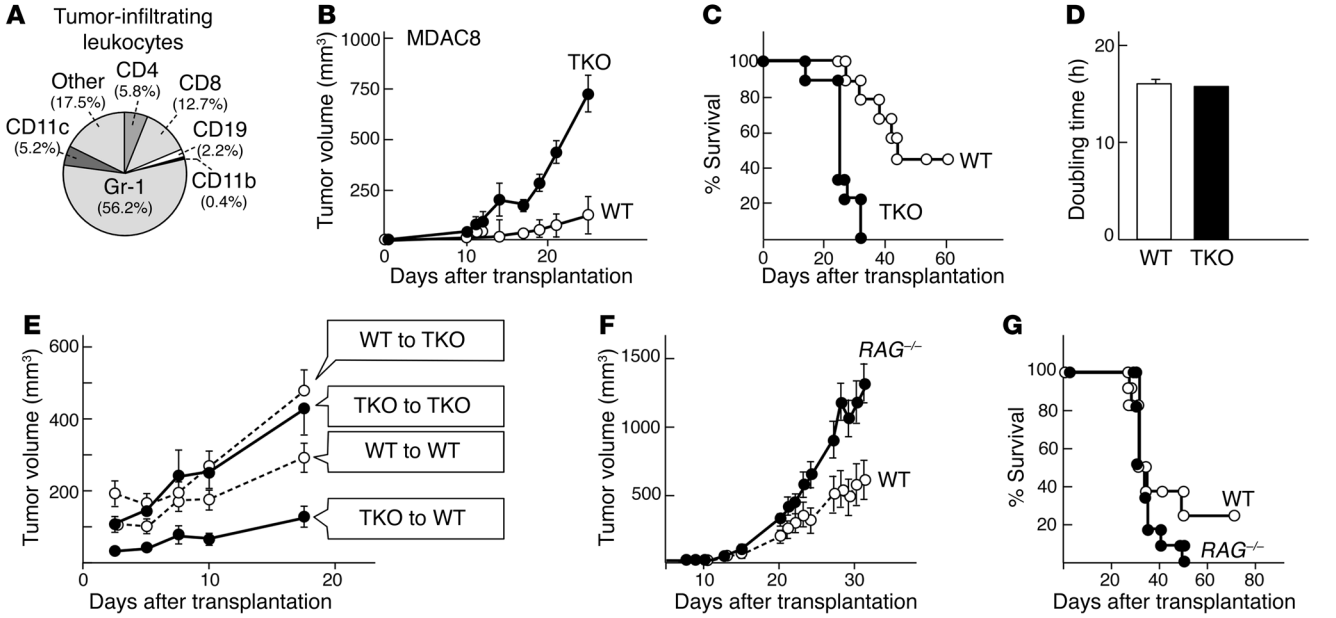

Figure 7

Growth of BALB/c TKO lung tumors is restricted in immunocompetent mice. (**A**) Analysis of tumor-infiltrating leukocytes by flow cytometry using the indicated antibodies; numbers are an average from 4 tumors harvested in 2 independent experiments. (**B** and **C**) 4×10^4 MDAC8 cells were transplanted subcutaneously into BALB/c WT or BALB/c TKO hosts. (**B**) Quantification of tumor size following transplantation. (**C**) Survival curve for mice following transplantation. (**D** and **E**) MDAC8 cells were harvested from either WT (MDAC8.WT) or TKO hosts (MDAC8.TKO). (**D**) 4×10^4 MDAC8.WT or MDAC8.TKO cells were plated in RPMI. Proliferation was measured by CTG; linear regression analysis on log-transformed data was used to calculate doubling time. (**E**) 4×10^4 MDAC8.WT or MDAC8.TKO cells were transplanted into WT or TKO hosts. (**F** and **G**) 4×10^4 MDAC8 cells were transplanted subcutaneously into BALB/c WT or BALB/c RAG KO hosts. (**F**) Quantification of tumor size following transplantation. (**G**) Survival curve for mice following transplantation. (**B**–**G**) Error bars represent SEM. Results are representative of at least 2 independent experiments with 8 to 12 mice per group.

tant diminished capacity to recognize and phagocytose apoptotic cells. These apoptotic cells then induce an inappropriate inflammatory reaction characterized by the production of inflammatory cytokines such as IL-6 and by Th17 skewing (23). This Th17 skewing may in fact contribute to IL-6 production in the pulmonary microenvironment, similar to the role of Th17 cells in IL-6 secretion recently described in two transplantable models of cancer (38). This early production of IL-6 in the pulmonary microenvironment is followed by autocrine secretion of IL-6 by the tumor cells. Autocrine IL-6 in turn plays an important role in optimal tumor growth, leading to activation of MAPK and STAT3 signaling. Although we do not know whether IL-6 serves a critical function in the early stages of tumorigenesis, these findings are suggestive. To fully explore the role of IL-6 and/or IL-17 in tumor formation, we would ideally cross the BALB/c TKO mice to an IL-6– or IL-17–deficient strain. However, given that BALB/c TKO RAG-KO mice were not viable beyond a few months due to severe immune deficiency, compounding the immune deficiency in TKO mice with loss of IL-6 and IL-17 may not be compatible with long-term survival.

An important role for IL-6 and downstream activation of STAT3 has been demonstrated in models of inflammation-associated liver and colon cancer (39–41), and activating mutations in the IL-6 receptor have been found in a subset of human hepatocellular carcinomas (42). In lung cancer, constitutive STAT3 activation is sufficient to promote tumor development and leads to chronic pulmonary inflammation, including activation of *Il6* gene expression (17). In human lung tumors, IL-6 has been identified as part of an autocrine growth loop in cancers expressing activating mutations in *EGFR* (15). While we have not observed EGFR activation in our system, this connection suggests that IL-6–driven growth may be a final common pathway for lung tumors generated through distinct mechanisms. Indeed, the lung tumor cell line LL, which does not produce IL-6 on its own, has recently been shown to activate IL-6 production in host macrophages through a Toll-like receptor–dependent mechanism following transplantation (43).

Multiple inflammatory signaling pathways appear to play a role in this system. As has been observed in other models of lung cancer, our findings suggest a critical function for NF-κB signaling in BALB/c TKO lung tumors. BALB/c TKO lung tumors show nuclear expression of both NF-κB1 and NF-κB2, and blocking NF-κB activation in vitro with IKK inhibitors leads to rapid tumor cell death. The autocrine secretion of IL-6 by these tumors also appears to derive in part from NF-κB activation, though the effects of NF-κB inhibition in BALB/c TKO tumors are not likely to be exerted through this mechanism alone, given that IL-6–knockdown cells remain viable.

In addition to establishing a model for inflammation-associated lung cancer, the tumors arising in BALB/c TKO mice present an intriguing system for studying the complicated interplay between protective antitumor immunity and inflammation-driven carcinogenesis. Antitumor immunity can limit tumor growth; however, chronic immune activation also leads to the induction of immune-regulatory responses that can promote tumorigenesis. Inflammatory cytokines, including IL-6, can induce myeloid-derived suppressor cell (MDSC) formation in the tumor microenviron-

ment, leading to the production of tumor growth factors as well as potent suppression of antitumor responses (32, 44). Although GM-CSF can function as a growth factor for MDSCs, this cytokine may not be absolutely required for their development, as cells with a surface phenotype similar to that of MDSCs with coexpression of Gr-1 and CD11b are readily detectable in GM-CSF–deficient mice (Figure 3 and our unpublished observations); however, whether the Gr-1$^+$CD11b$^+$ cells identified in GM-CSF–deficient animals are true MDSCs possessing immune-suppressive function remains to be studied. In addition to MDSCs, recent work has linked inflammation and failure of adaptive antitumor immunity to models of chemically induced skin cancer; however, whether inflammation and failure of antitumor immunity contribute to the growth of the same tumors in these models remains unclear (45).

The role of the immune response in human lung cancer is still incompletely understood; however, expression of known tumor antigens, such as MAGE-A3, has been found in many NSCLCs (46). A variety of vaccination approaches have been used to elicit immune responses against established lung tumors, and a single-antigen vaccine against MAGE-A3 is now undergoing testing in a phase III trial (46).

We have shown a dual role for the immune system in BALB/c TKO lung tumors. These lung tumors occur in a microenvironment of chronic inflammation and infection, and the inflammatory cytokine IL-6 acts as an autocrine tumor growth factor even in advanced tumors. Yet failure of antitumor immunity also appears to influence the growth of these tumors: the same tumors that are driven by IL-6 are readily transplantable into other immunodeficient hosts, including mice lacking adaptive immunity, but can be rejected by wild-type animals. This rejection is likely due to the recognition of tumor antigens by the immune system and is consistent with the well-established role for IFN-γ in mediating adaptive antitumor immune responses and immune editing (36, 37). Further consistent with an immune editing model, transplanted tumors that escape in wild-type hosts no longer show growth inhibition during subsequent transplantation into immunocompetent animals, indicating that loss of immunogenicity is an important step in the growth of these tumors after transplantation. In addition to loss of IFN-γ–dependent immune responses in BALB/c TKO mice, IL-6 production and STAT3 activation during chronic pulmonary inflammation may further suppress antitumor responses, as STAT3 activation in the tumor microenvironment leads to suppression of both innate and adaptive immunity, in addition to its direct role in tumorigenesis (47).

Collectively, these findings establish a distinct model of lung cancer, dependent on alterations in immune function, leading to both tumor-promoting inflammation and failure of antitumor immunity. Understanding the molecular mechanisms that separate tumor-promoting inflammation from antitumor immunity in BALB/c TKO lung tumor development may provide insights into inflammation-associated malignancies and contribute to the generation of immune therapies for these cancers.

Methods

Animals. BL6 and BALB/c wild-type mice were purchased from Taconic or The Jackson Laboratory or bred in-house. IFN-γ–deficient mice were purchased from Taconic. Combined cytokine-deficient mice were generated in-house and backcrossed to BALB/c for more than 10 generations. TKO RAG-KO mice were generated by crossing TKO mice to RAG-2–deficient mice purchased from Taconic. All animal experimentation was done in accordance with institutional guidelines and the review board of Harvard Medical School, which granted permission for this study, and was approved by the Association for Assessment and Accreditation of Laboratory Animal Care–accredited Dana-Farber Cancer Institute IACUC.

Pathology. Tissues were fixed in 10% neutral buffered formalin, processed routinely, and embedded in paraffin. Immunohistochemistry was performed using standard techniques with monoclonal antibodies to SPC (Chemicon) and pERK (Cell Signaling Technology).

Analysis of BAL fluid. BAL was performed by injection of 700 μl sterile PBS directly into the trachea of mice. Fluid was extracted and used for subsequent analysis. Cytokines were measured directly using fluorescently labeled anti-cytokine beads (Beadlyte 21-plex Cytokine Detection System; Upstate, Millipore). Viable cell counts were determined by trypan blue exclusion, and immune phenotyping was performed using flow cytometry.

Flow cytometry and immunoblotting. Single-cell suspensions were made from resected tumors by treatment with 1% collagenase (Sigma-Aldrich), or from resected spleens by mechanical disruption; red blood cells were removed by hypotonic lysis. Cells were then washed and stained for 30 minutes on ice with the indicated antibodies in PBS with 1% inactivated fetal calf serum. The following antibodies were used for flow cytometry and purchased from BD: CD3, CD4, CD8, CD11b, CD11c, CD19, and Gr-1. For Western blot analysis, tumor cells were lysed using the NE-PER Nuclear and Cytoplasmic Extraction Reagent (Pierce). Protein concentration was quantified by BCA assay (Pierce), and 30 μg protein was loaded per lane onto 12% acrylamide gels. SDS-PAGE was followed by transfer to nitrocellulose and immunoblotting using the indicated primary antibodies. Secondary antibodies conjugated to alkaline phosphatase were purchased from Jackson ImmunoResearch Laboratories Inc. and used at 1:10,000 dilution. STAT3, pERK, p52, p65, RelB, and β-actin antibodies were from Cell Signaling Technology. USF-2 antibody was from Santa Cruz Biotechnology Inc.

T cell stimulation. T cells were stimulated for 72 hours using plate-bound anti-CD3 (hamster mAb clone 145-2C11; BD) and anti-CD28 (hamster mAb clone 37.15; BD).

Cytokine measurements. Cytokines were measured by ELISA or by multi-cytokine bead array as indicated; both techniques were performed according to the manufacturer's instructions. IL-6 and MCP-1 ELISA kits were from BD; IL-17 and VEGF kits were from R&D Systems. Multi-cytokine beads were from Upstate (BAL fluid, tumor cytokine secretion, T cell assay) or from Millipore (macrophages, IL-6 knockdown, IKK inhibitor assay).

Lentiviral knockdown. 1×10^4 tumor cells were infected by spin transduction with highly concentrated lentiviral particles (Broad Institute, Sigma-Aldrich) using an MOI of 15. Puromycin (5 μg/ml) was added 48 hours following infection. Cells were analyzed beginning 1 week after puromycin initiation. The sequences for the shRNA encoded by each of the lentiviruses used were as follows: for IL-6 KD-1, the shRNA encoded GCAATGGCAATTCTGATTGTACTCGAGTACAATCAGAATTGCCATTGC; for IL-6 KD-2, the shRNA encoded CCAGAGTCCTTCAGAGAGATACTCGAGTATCTCTCTGAAGGACTCTGG.

Bone marrow transplantation experiments. Bone marrow was harvested from wild-type or TKO mice by aspiration of femurs. Two-month-old recipient mice were irradiated using 6 Gy and reconstituted with 1×10^7 donor marrow cells per mouse via tail vein injection. Reconstituted mice were monitored and given acidified drinking water for 21 days and then observed until 1 year of age.

Tumor challenge experiments. MDAC tumor lines were developed from resected primary lung tumors. Primary tumors were mechanically disrupted and reinjected subcutaneously or intravenously into naive TKO hosts and monitored for growth. After serial passage through 3 TKO hosts, tumors were isolated, digested with 1% collagenase to obtain a single-cell suspension, and cultured in RPMI containing 10% serum, or maintained through serial transplantation. For tumor transplantation, tumor cells were injected subcutaneously. All

tumor-bearing mice were monitored for signs of morbidity and were sacrificed when body weight dropped more than 10% or when tumors reached a critical size. IL-6 production from ex vivo isolated tumor cells was determined by isolating tumors from secondary hosts and culturing them at 1×10^4 cells/ml in RPMI; IL-6 was measured in culture supernatants after 72 hours. IL-6 production was compared with baseline IL-6 production from cell lines that were frozen at the time of transplantation and thawed 1 week before analysis.

Statistics. Two-sample comparisons used the 2-tailed *t* test with pooled variance if there was no evidence of inhomogeneity of variances between groups. If the variances were unequal, the exact Wilcoxon rank-sum test, a nonparametric alternative to the *t* test, was used. Every effort was made to keep testing consistent across related experiments. For comparisons of more than 2 groups, ANOVA was used if there was no evidence of inhomogeneity of variance; the Kruskal-Wallis test was the nonparametric alternative. Tumor growth studies were analyzed using mixed-model ANOVA. A *P* value less than 0.05 was considered statistically significant for all comparisons.

Acknowledgments

We thank Stephen Conley of Massachusetts General Hospital for help with photography. This work was supported by National Institute on Aging grant F30AG030298 and the Margaret A. Cunningham Immune Mechanisms of Cancer Research Fellowship (to M. Dougan); the American Lung Association, United Against Lung Cancer, and NIH grants R01 CA122794 and R01 CA140594 (to K.-K. Wong); and NIH grant R01 CA143083 (to G. Dranoff).

Received for publication August 17, 2010, and accepted in revised form March 2, 2011.

Address correspondence to: Glenn Dranoff, Dana-Farber Cancer Institute, Dana 520C, 44 Binney Street, Boston, Massachusetts 02115, USA. Phone: 617.632.5051; Fax: 617.632.5167; E-mail: glenn_dranoff@dfci.harvard.edu.

1. Jemal A, et al. Cancer statistics, 2008. *CA Cancer J Clin*. 2008;58(2):71–96.
2. Travis WD, Travis LB, Devesa SS. Lung cancer. *Cancer*. 1995;75(1 suppl):191–202.
3. Doll SR. Smoking and lung cancer. *Am J Respir Crit Care Med*. 2000;162(1):4–6.
4. Kuper H, Adami HO, Boffetta P. Tobacco use, cancer causation and public health impact. *J Intern Med*. 2002;251(6):455–466.
5. Herbst RS, Heymach JV, Lippman SM. Lung cancer. *N Engl J Med*. 2008;359(13):1367–1380.
6. Meuwissen R, Berns A. Mouse models for human lung cancer. *Genes Dev*. 2005;19(6):643–664.
7. Kim CF, et al. Mouse models of human non-small-cell lung cancer: raising the bar. *Cold Spring Harb Symp Quant Biol*. 2005;70:241–250.
8. Johnson L, et al. Somatic activation of the K-ras oncogene causes early onset lung cancer in mice. *Nature*. 2001;410(6832):1111–1116.
9. Ji H, et al. The impact of human EGFR kinase domain mutations on lung tumorigenesis and in vivo sensitivity to EGFR-targeted therapies. *Cancer Cell*. 2006;9(6):485–495.
10. Dougan M, Dranoff G. Immune therapy for cancer. *Annu Rev Immunol*. 2009;27:83–117.
11. Malkinson AM. Role of inflammation in mouse lung tumorigenesis: a review. *Exp Lung Res*. 2005; 31(1):57–82.
12. Takahashi H, Ogata H, Nishigaki R, Broide DH, Karin M. Tobacco smoke promotes lung tumorigenesis by triggering IKKbeta- and JNK1-dependent inflammation. *Cancer Cell*. 2010;17(1):89–97.
13. Karin M, Greten FR. NF-kappaB: linking inflammation and immunity to cancer development and progression. *Nat Rev Immunol*. 2005;5(10):749–759.
14. Schreinemachers DM, Everson RB. Aspirin use and lung, colon, and breast cancer incidence in a prospective study. *Epidemiology*. 1994;5(2):138–146.
15. Gao SP, et al. Mutations in the EGFR kinase domain mediate STAT3 activation via IL-6 production in human lung adenocarcinomas. *J Clin Invest*. 2007;117(12):3846–3856.
16. Yu H, Pardoll D, Jove R. STATs in cancer inflammation and immunity: a leading role for STAT3. *Nat Rev Cancer*. 2009;9(11):798–809.
17. Li Y, Du H, Qin Y, Roberts J, Cummings OW, Yan C. Activation of the signal transducers and activators of the transcription 3 pathway in alveolar epithelial cells induces inflammation and adenocarcinomas in mouse lung. *Cancer Res*. 2007;67(18):8494–8503.
18. Barbie DA, et al. Systematic RNA interference reveals that oncogenic KRAS-driven cancers require TBK1. *Nature*. 2009;462(7269):108–112.
19. Houghton AM, et al. Neutrophil elastase-mediated degradation of IRS-1 accelerates lung tumor growth. *Nat Med*. 2010;16(2):219–223.
20. Meylan E, et al. Requirement for NF-kappaB signalling in a mouse model of lung adenocarcinoma. *Nature*. 2009;462(7269):104–107.
21. Deng J, et al. Knockout of the tumor suppressor gene Gprc5a in mice leads to NF-kappaB activation in airway epithelium and promotes lung inflammation and tumorigenesis. *Cancer Prev Res (Phila)*. 2010;3(4):424–437.
22. Enzler T, et al. Deficiencies of GM-CSF and interferon gamma link inflammation and cancer. *J Exp Med*. 2003;197(9):1213–1219.
23. Jinushi M, Nakazaki Y, Dougan M, Carrasco DR, Mihm M, Dranoff G. MFG-E8-mediated uptake of apoptotic cells by APCs links the pro- and anti-inflammatory activities of GM-CSF. *J Clin Invest*. 2007;117(7):1902–1913.
24. Enzler T, et al. Functional deficiencies of granulocyte-macrophage colony stimulating factor and interleukin-3 contribute to insulitis and destruction of beta cells. *Blood*. 2007;110(3):954–961.
25. Manenti G, et al. Mouse genome-wide association mapping needs linkage analysis to avoid false-positive Loci. *PLoS Genet*. 2009;5(1):e1000331.
26. Street SE, Trapani JA, MacGregor D, Smyth MJ. Suppression of lymphoma and epithelial malignancies effected by interferon gamma. *J Exp Med*. 2002;196(1):129–134.
27. Huffman JA, Hull WM, Dranoff G, Mulligan RC, Whitsett JA. Pulmonary epithelial cell expression of GM-CSF corrects the alveolar proteinosis in GM-CSF-deficient mice. *J Clin Invest*. 1996;97(3):649–655.
28. Becker C, et al. TGF-beta suppresses tumor progression in colon cancer by inhibition of IL-6 transsignaling. *Immunity*. 2004;21(4):491–501.
29. El-Omar EM, et al. Interleukin-1 polymorphisms associated with increased risk of gastric cancer. *Nature*. 2000;404(6776):398–402.
30. Steinman L. A brief history of T(H)17, the first major revision in the T(H)1/T(H)2 hypothesis of T cell-mediated tissue damage. *Nat Med*. 2007; 13(2):139–145.
31. Langowski JL, et al. IL-23 promotes tumour incidence and growth. *Nature*. 2006;442(7101):461–465.
32. DeNardo DG, et al. CD4(+) T cells regulate pulmonary metastasis of mammary carcinomas by enhancing protumor properties of macrophages. *Cancer Cell*. 2009;16(2):91–102.
33. Gounaris E, et al. T-regulatory cells shift from a protective anti-inflammatory to a cancer-promoting proinflammatory phenotype in polyposis. *Cancer Res*. 2009;69(13):5490–5497.
34. Paez-Ribes M, et al. Antiangiogenic therapy elicits malignant progression of tumors to increased local invasion and distant metastasis. *Cancer Cell*. 2009;15(3):220–231.
35. Ebos JM, Lee CR, Cruz-Munoz W, Bjarnason GA, Christensen JG, Kerbel RS. Accelerated metastasis after short-term treatment with a potent inhibitor of tumor angiogenesis. *Cancer Cell*. 2009; 15(3):232–239.
36. Dunn GP, Old LJ, Schreiber RD. The three Es of cancer immunoediting. *Annu Rev Immunol*. 2004; 22:329–360.
37. Koebel CM, et al. Adaptive immunity maintains occult cancer in an equilibrium state. *Nature*. 2007; 450(7171):903–907.
38. Wang L, Yi T, Kortylewski M, Pardoll DM, Zeng D, Yu H. IL-17 can promote tumor growth through an IL-6-Stat3 signaling pathway. *J Exp Med*. 2009; 206(7):1457–1464.
39. Grivennikov S, et al. IL-6 and stat3 are required for survival of intestinal epithelial cells and development of colitis-associated cancer. *Cancer Cell*. 2009; 15(2):103–113.
40. Bollrath J, et al. gp130-mediated Stat3 activation in enterocytes regulates cell survival and cell-cycle progression during colitis-associated tumorigenesis. *Cancer Cell*. 2009;15(2):91–102.
41. Naugler WE, et al. Gender disparity in liver cancer due to sex differences in MyD88-dependent IL-6 production. *Science*. 2007;317(5834):121–124.
42. Rebouissou S, et al. Frequent in-frame somatic deletions activate gp130 in inflammatory hepatocellular tumours. *Nature*. 2009;457(7226):200–204.
43. Kim S, et al. Carcinoma-produced factors activate myeloid cells through TLR2 to stimulate metastasis. *Nature*. 2009;457(7225):102–106.
44. Ostrand-Rosenberg S, Sinha P. Myeloid-derived suppressor cells: linking inflammation and cancer. *J Immunol*. 2009;182(8):4499–4506.
45. Swann JB, et al. Demonstration of inflammation-induced cancer and cancer immunoediting during primary tumorigenesis. *Proc Natl Acad Sci U S A*. 2008; 105(2):652–656.
46. Brichard VG, Lejeune D. GSK's antigen-specific cancer immunotherapy programme: pilot results leading to Phase III clinical development. *Vaccine*. 2007; 25 suppl 2:B61–B71.
47. Yu H, Kortylewski M, Pardoll D. Crosstalk between cancer and immune cells: role of STAT3 in the tumour microenvironment. *Nat Rev Immunol*. 2007; 7(1):41–51.